Talanta 161 (2016) 681–685

Contents lists available at ScienceDirect

Talanta

journal homepage: www.elsevier.com/locate/talanta

Efficient enrichment of glycopeptides with sulfonic acid-functionalized mesoporous silica

Aisha Bibi, Huangxian Ju *

State Key Laboratory of Analytical Chemistry for Life Science, School of Chemistry and Chemical Engineering, Nanjing University, Nanjing 210023, PR China

ARTICLE INFO

Article history:
Received 19 July 2016
Received in revised form
31 August 2016
Accepted 3 September 2016

Keywords:
Mesoporous silica
Sulfonic acid-functionalized mesoporous silica
Selective enrichment
Glycopeptides
Matrix-assisted laser desorption/ionization mass spectrometry

ABSTRACT

This work presents an efficient and selective enrichment method for glycoprotein/glycopeptides with sulfonic acid-functionalized mesoporous silica (SBA-15-SO_3H), which is synthesized via simple oxidation of -SH groups with H_2O_2. The functionalized SBA-15 shows large surface area and accessible pores, and can selectively adsorb glycopeptides via hydrogen bond and hydrophilic interaction. Upon the selective enrichment prior to the mass spectrometric (MS) analysis, the signals of glycopeptides are significantly enhanced, which leads to the identifiable signals of 21 glycopeptides from the digest of HRP, 16 glycopeptides from the digest of human IgG, and 16 glycopeptides from the digest of chicken avidin. The SBA-15-SO_3H gives significant selectivity for glycopeptides even at a low molar ratio of glycopeptides to nonglycopeptides with an enrichment time of 15 min. Therefore, this work provides a powerful material for selective enrichment and identification of low abundant glycopeptides in glycoproteomic analysis.

1. Introduction

Protein glycosylation is one of the most vital post-translational modifications and commonly links with regulation of cell division, tumor immunology, inflammation, and protein-protein interactions [1–8]. Therefore, glycoprotein research has important biological significance. The detection of the glycosylated sites of proteins plays crucial roles in diverse biological processes and discovery of new targets for drugs at molecular level [9,10]. Currently mass spectrometry (MS) coupled with matrix-assisted laser desorption/ionization (MALDI) or electrospray ionization (ESI) has become benchmark analytical techniques for the determination of glycoprotein. However, these techniques are generally lack of the sensitivity demanded for low abundant glycopeptides, and the ion suppression effect caused by the co-presence of non-glycosylated peptides often decreases the ionization efficiency [11,12]. Thus, an enrichment step prior to MS detection is important for the analysis of glycoproteins to improve the detection sensitivity. As a result, it is necessary to develop efficient enrichment methods for detailed glycoproteomic studies [13–15].

Several methods or materials have been reported to enrich glycopeptides, including the application of lectin [16], boronic acid [11,17], hydrazine beads [18], magnetic beads [19,20] and gold nanoparticles [21], immobilized metal affinity chromatography [22], size-exclusion chromatography [23], and hydrophilic interaction chromatography with solid phase extraction (HIC-SPE) [24]. The HIC adsorbents have also been applied for isolation of glycopeptides from digests of purified glycoproteins and more complex protein mixtures using sepharose, cellulose, saccharides, zwitterionic beads and metal–organic frameworks [25–29]. These methods are sensitive but have limitations in selectivity. To solve this problem, boronic acid modified nanomaterials have been reported for selective enrichment [11,17,32] and solid-phase extraction [30–33] of glycopeptides. The boronic-based chemically selective strategy shows much improved selectivity for enrichment and isolation of glycopeptides and enhanced sensitivity for MS analysis of glycopeptides.

Here, we use sulfonic acid-functionalized mesoporous silica (SBA-15-SO_3H) to develop a method for selective enrichment of glycopeptides via hydrogen bond and hydrophilic interaction, and then convenient elution to perform following MS analysis (Scheme 1). The functionalization of SBA-15 can conveniently be performed by immobilizing 3-mercaptopropyl trimethoxysilane (MPTMS) on SBA-15 and then oxidizing the -SH groups with H_2O_2 to form active sulfonic acid groups [34] (Fig. 1). The porous structure of SBA-15 with abundant sulfonic groups assures the adsorption selectivity and capacity of glycopeptides. Thus the proposed strategy shows high sensitivity for detection of glycopeptides from the digests of different glycoproteins. The SBA-15-SO_3H provides promising application in selective enrichment and identification of glycopeptides for glycoproteomic research.

* Corresponding author.
E-mail address: hxju@nju.edu.cn (H. Ju).

http://dx.doi.org/10.1016/j.talanta.2016.09.012
0039-9140/

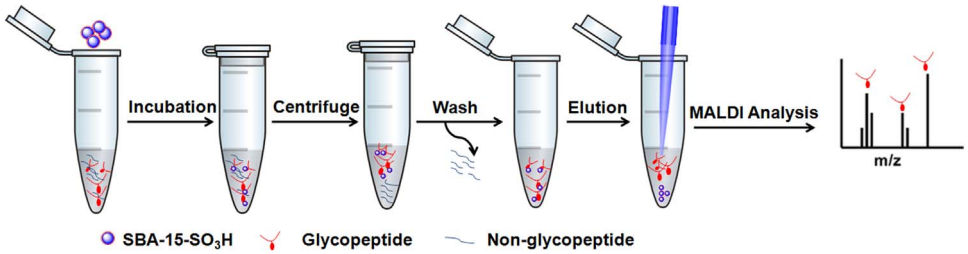

Scheme 1. Workflow of specific enrichment with SBA-15-SO_3H and MALDI-MS analysis of glycopeptides.

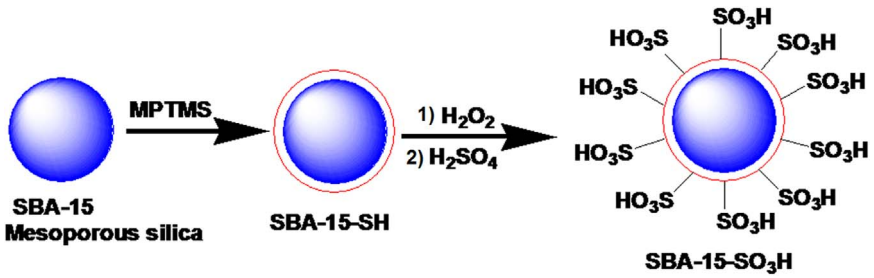

Fig. 1. Synthesis of SBA-15-SO_3H.

2. Experimental

2.1. Materials and reagents

Horseradish peroxidase (HRP, MW ~44 kDa), bovine serum album (BSA, MW ~66 kDa), human serum immunoglobulin G (human IgG), chicken avidin, trypsin (from bovine pancreas, ≥ 10,000 BAEE units mg^{-1}), ammoniumbicarbonate (NH_4HCO_3), DL-dithiothreitol (DTT), iodoacetamide (IAA), trifluoroacetic acid (TFA, ≥ 90%), α-cyano-4-hydroxycinnamic acid (CHCA) and MPTMS ≥ 90% were purchased from Sigma-Aldrich Inc. (USA). Sulfuric acid, anhydrous toluene, dichloromethane, ethyl acetate, hydrogen peroxide and methanol were obtained from Shanghai Reagent Company (Shanghai, China). All these reagents were used without further purification. Ultrapure water obtained from a Millipore water purification system (≥ 18 MΩ, Milli-Q, Millipore) was used in all experiments.

2.2. Apparatus

Fourier-transform infrared (FT-IR) spectra were recorded on Thermo Nicolet 380 spectrometer using KBr pellets (Thermo Nicolet, Wisconsin, USA). Zeta potential analysis was performed on a Zetasizer instrument (Nano-Z, Malvern, UK). X-ray powder diffraction data was recorded using an X-Ray Powder Diffractometer (Bruker AXS Ltd, Germany). Nitrogen absorption/desorption measurement was performed on a porosimeter (ASAP 2020, Micromeritics, USA).

2.3. Preparation of SBA-15-SO_3H

Mesoporous silica (SBA-15) was firstly synthesized according to the procedure reported previously [35]. The obtained SBA-15 was dried in oven at 150 °C, overnight under vacuum to remove absorbed water. The functionalization of SBA-15 with -SH groups was carried out by mixing 4 g of dried SBA-15 and 1.45 g of MPTMS in 460 ml of anhydrous toluene, which was vigorously stirred and refluxed for 24 h [34]. The solid product was recovered by filtration and added a mixture containing 151 ml dichloromethane and 223 ml ethyl acetate. The mixture was stirred and refluxed for more 24 h. After filtration, the thiol modified SBA-15 was obtained.

The thiol modified SBA-15 (4 g) was then dispersed in a mixture containing 25 ml H_2O_2, 108 ml CH_3OH and 286 ml H_2O. The resulting solution was stirred at room temperature for 12 h and filtered. The desired solid product was dispersed in 200 ml of 0.5 M H_2SO_4 and stirred at room temperature for 12 h. The solid product was then filtered, washed thrice with ethanol and water, and dried overnight under vacuum oven at 100 °C to obtain SBA-15-SO_3H.

2.4. Digestion of proteins

HRP as a model glycoprotein was firstly dissolved in NH_4HCO_3 buffer (50 mM, pH 8.3) to a final concentration of 1 mg ml^{-1} and denatured at 100 °C for 5 min. The solution was incubated with trypsin at an enzyme-to-protein ratio of 1:40 (w/w) at 37 °C for 16 h. The digestion of human IgG, chicken avidin and BSA was performed by incubating the mixture of 50 μL of 200 mM DTT and 1 ml of 1 mg ml^{-1} protein in 50 mM NH_4HCO_3 buffer (50 mM, pH 8.3) at 100 °C for 5 min. After the mixture was cooled down to room temperature, 40 μL of 1 M IAA was added in dark for 45 min, and the excessive IAA was consumed with 200 μL of 200 mM DTT at room temperature for 1 h. Then, trypsin was added to the protein solution at an enzyme-to-protein ratio of 1:40 (w/w) and incubated at 37 °C for 16 h. Finally, 0.5% FA was used to stop the digest reaction. The obtained samples were stored at −20 °C prior to enrichment.

2.5. Enrichment of glycopeptides

SBA-15-SO_3H (1 mg) was dispersed in 100 μL ACN/H_2O/TFA (88:11.9:0.1, v/v/v), and mixed with 100 μL sample of digested glycoprotein to incubate with shaking at room temperature for 15 min. The glycopeptide-loaded SBA-15-SO_3H was collected by centrifugation at 14,000 rpm for 3 min, and washed three times with 100 μL ACN/H_2O/TFA (88:11.9:0.1, v/v/v) to remove the non-specifically adsorbed peptides. Then, 20 μL of ACN/H_2O/TFA (50:49:1, v/v/v) was added to release the captured glycopeptides from SBA-15-SO_3H over a period of 30 min.

2.6. MALDI-TOF MS analysis

Equivalent amounts (0.5 μL) of the elute and saturated CHCA solution in ACN/H_2O/TFA (60:39.9:0.1, v/v/v) as the matrix were

sequentially dropped onto the MALDI plate for MS analysis. All mass spectra were accorded on a 4800 *Plus* MALDI TOF/TOF Analyzer (AB Sciex, USA) with a Nd% YAG laser at 355 nm, a repetition rate of 200 Hz and an acceleration voltage of 20 kV.

3. Results and discussion

3.1. Characterization of SBA-15-SO_3H

The FT-IR spectra of both SBA-15 and SBA-15-SO_3H showed a broad absorption band around 3448 cm^{-1} (Fig. S1A), indicating the –OH stretching vibration. The band at 1637 cm^{-1} and the sharp bands around 967 and 806 cm^{-1} at the FT-IR spectrum of SBA-15 were attributed to the –OH deformation. The FT-IR spectrum of SBA-15-SO_3H exhibited two bands centered at 2928 and 2854 cm^{-1}, which were corresponded to C-H stretching [36]. After functionalization with sulfonic acid, the mesoporous silica became more negatively charged (Fig. S1B). The low-angle XRD pattern of the synthesized SBA-15-SO_3H displayed three well-resolved peaks (Fig. S2), which were indexed to (100), (101) and (200) reflections, respectively. These results suggested that the hexagonal mesoporous structure of SBA-15-SO_3H [37]. The nitrogen adsorption-desorption isotherm of the SBA-15-SO_3H showed an average pore diameter of 4.8 nm (Fig. S3), and the surface area and pore volume were calculated to be 520 $m^2\ g^{-1}$ and 0.60 $cm^3\ g^{-1}$ using the BET and BJH model on the adsorption branch of the isotherm, respectively.

3.2. Specific enrichment of glycopeptides

A tryptic HRP digest was employed as the test sample to estimate the enrichment capability and specificity of SBA-15-SO_3H according to the procedure described in Scheme 1. The enrichment (incubation) time with 5 ng μL^{-1} SBA-15-SO_3H was firstly optimized. At an incubation time of 3 min, the mass spectrum for 10 ng μL^{-1} HRP showed only 9 peaks corresponding to different glycopeptides, while it exhibited 21 glycopeptides at the incubation time of 15 min (Fig. S4), which was much shorter than 2 h for the enrichment using boronic acid functionalized magnetic carbon nanotubes to obtain the signals of 21 glycopeptides [32], and 1 h for the enrichment with affinity chromatography supported by concanavalin A functionalized magnetic particles [19]. It could be ascribed to the high surface area, large pore size and high affinity of SBA-15-SO_3H to glycopeptides due to the formation of hydrogen bond and hydrophilic interaction.

The specificity of SBA-15-SO_3H toward glycopeptides was investigated with the tryptic digest of 10 ng μL^{-1} HRP by MALDI-TOF mass spectra. In the absence of enrichment, only 6 glycopeptide peaks (1, 3, 17, 18, 20 and 21) with weak intensity and low signal-to-noise ratio (S/N) were observed (Fig. 2A). Moreover, low abundance of glycopeptides and strong signal suppression by the abundant of non-specific peptides dominated in the spectrum. After enrichment with SBA-15-SO_3H for 15 min, the high background from non-specific peptides disappeared, and the mass spectrum showed clear 21 signals corresponding to glycopeptides (Fig. 2B). The performance of SBA-15-SO_3H and detectable peaks of the glycopeptides were superior to previously reported boronic acid functionalized mesoporous silica (5) [11], core-shell structure Fe_3O_4@C@Au magnetic microspheres (14) [38], mercaptophenylboronic acid modified gold nanoparticles@silica bubbles (19) [39], and boronic acid functionalized core-satellite composite nanoparticles (17) [31].

The performance of SBA-15-SO_3H for enrichment of glycopeptides was further tested using the tryptic digest of human IgG. Similarly, the mass spectrum without enrichment showed the non-

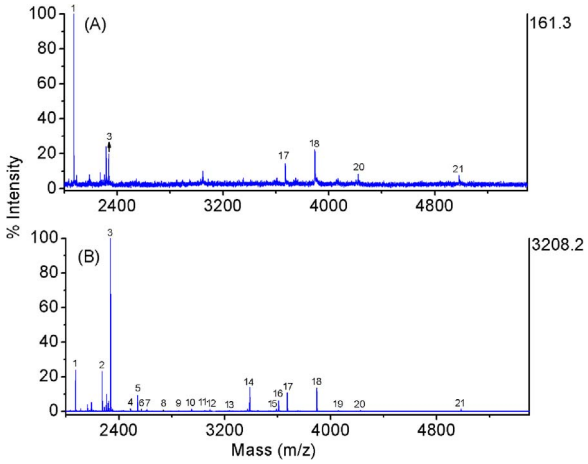

Fig. 2. Mass spectra of tryptic digests of 10 ng μL^{-1} HRP (A) without and (B) with enrichment using 5 ng μL^{-1} SBA-15-SO_3H for 15 min.

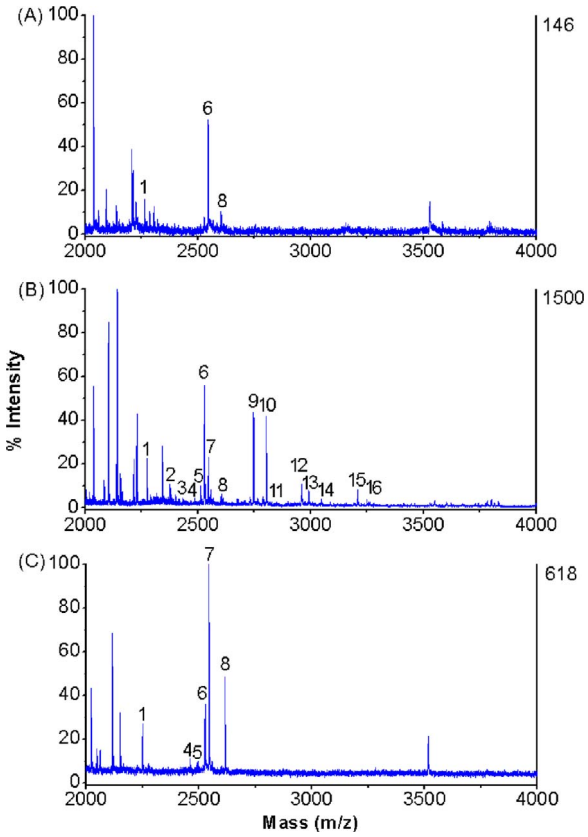

Fig. 3. Mass spectra of tryptic digests of human IgG (A) without and (B), (C) with enrichment using (B) 5 and (C) 2.5 ng μL^{-1} SBA-15-SO_3H for 15 min.

glycopeptide peaks, which led to high background for detection of glycopeptides, and only three glycopeptide peaks could be identified (Fig. 3A). In contrast, after enrichment with 5.0 ng μL^{-1} SBA-15-SO_3H for 15 min, the mass spectrum showed 16 glycopeptide peaks with over 10 times higher intensity (Fig. 3B). The detailed information of the identified glycopeptides from tryptic digests of HRP and human IgG were listed in Tables S1 and S2. The detectable peak number was more than those previously reported boronic acid functionalized mesoporous silica [11]. Obviously, both the number of detectable glycopeptides and the peak intensity depended on the concentration of SBA-15-SO_3H used for enrichment. At the same incubation time, the enrichment with 2.5 ng μL^{-1} SBA-15-SO_3H produced only 6 glycopeptide peaks (Fig. 3C).

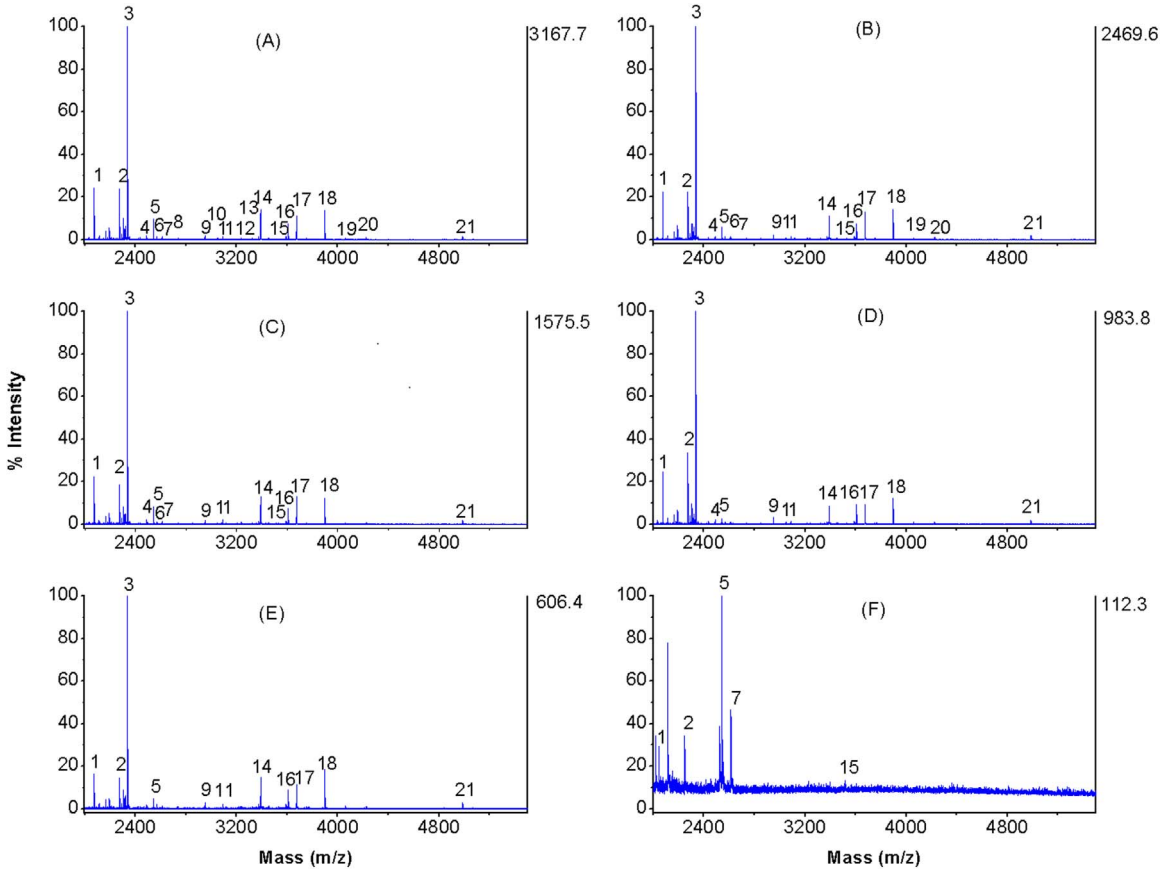

Fig. 4. Mass spectra of (A) 10, (B) 5, (C) 2, (D) 1, (E) 0.2, and (F) 0.1 ng μL^{-1} HRP digests after enrichment with 5 ng μL^{-1} SBA-15-SO_3H for 15 min.

3.3. Sensitivity of glycopeptide identification

To evaluate the detection sensitivity, the tryptic digests of HRP at different concentrations were enriched with 5.0 ng μL^{-1} SBA-15-SO_3H for 15 min. The mass spectra showed 21, 17, 15, 12 and 11 peaks at the concentrations of 10, 5.0, 2.0, 1.0 and 0.2 ng μL^{-1} respectively, with decreasing intensity and signal-to-noise ratio (S/N) (Fig. 4). When the concentration further decreased, the number of detectable peaks abruptly decreased, and only 5 glycopeptide peaks could be identified at 0.1 ng μL^{-1} (Fig. 4F), which could be considered as the detection limit, and was comparable with the previous report using boronic acid functionalized magnetic carbon nanotubes [32], and mercaptophenylboronic acid modified gold nanoparticles@silica bubbles [39]. The detection limit was 10 times lower than that of 1 ng μL^{-1} with boronic acid functionalized core-shell polymer nanoparticles [40].

The high sensitivity led to its wide practicability for glycopeptide identification of different proteins. Using the tryptic digest of chicken avidin as an example, after enrichment with SBA-15-SO_3H the mass spectrum showed 16 glycopeptide peaks at the chicken avidin concentration of 2 pg μL^{-1} (Fig. 5B, and Table S3), while only three glycopeptide peaks could be identified in the absence of enrichment (Fig. 5A), confirming the promising application of SBA-15-SO_3H for the capture of glycopeptides.

3.4. Specificity of glycopeptide enrichment

The enhanced hydrogen bond and hydrophilic interaction between SBA-15-SO_3H and glycopeptides greatly improved the efficiency of specific enrichment toward glycopeptides. The enrichment specificity of SBA-15-SO_3H toward glycopeptides was further examined with the tryptic digests of HRP/BSA mixtures at the ratios of 1:1 and 1:100. After enrichment with SBA-15-SO_3H, the presence of highly abundant non-glycopeptides in the tryptic digests did not suppress the signals of glycopeptides (Fig. 6). Moreover, the increased amount of non-glycopeptides did not obviously influence the relative intensity of glycopeptide peaks, and 8 glycopeptides could be identified from the mixture of HRP and BSA at the ratio of 1:100, which was much better than three glycopeptide peaks when using boronic acid-functionalized mesoporous silica (MCM-41-APTES-CPB) for enrichment [41]. Therefore, SBA-15-SO_3H demonstrated better performance for enrichment of glycopeptides in complex samples.

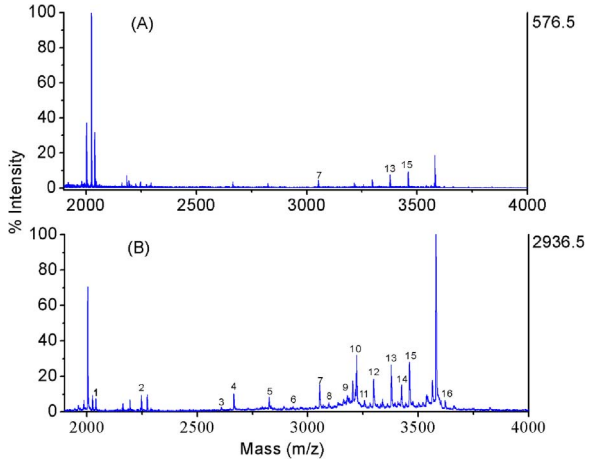

Fig. 5. Mass spectra of tryptic digests of 2 pg μL^{-1} chicken avidin (A) without and (B) with enrichment using 5 ng μL^{-1} SBA-15-SO_3H for 15 min.

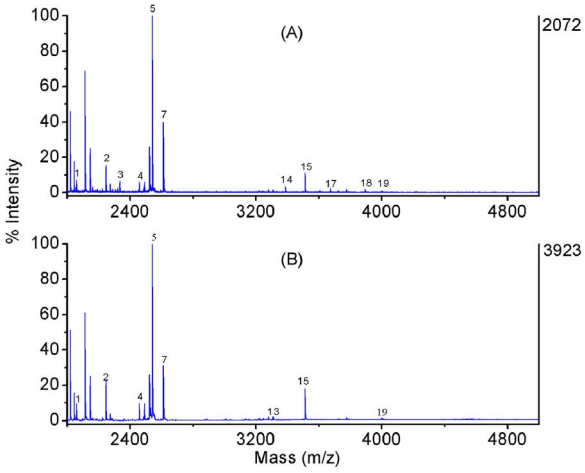

Fig. 6. Mass spectra of tryptic digests of mixtures of HRP and BSA at (A) 1:1 and (B) 1:100 upon enrichment with 5 ng μL^{-1} SBA-15-SO_3H for 15 min.

4. Conclusions

The sulfonic acid-functionalized mesoporous silica (SBA-15-SO_3H) can be conveniently preapred for efficient enrichment of glycopeptides, which shows high capacity due to the porous structure and large surface area. The abundant sulfonic groups on SBA-15-SO_3H surface lead to good adsorption selectivity toward glycopeptides through hydrogen bond and hydrophilic interaction. Upon the enrichment step with relatively short incubation time, much more glycopeptide peaks from various digests of glycoproteins can be identified, which shows high signal-to-background ratio and leads to high detection sensitivity. Although this proposed method cannot be used for quantitative analysis of these glycopeptides due to the "sweet spots" effect produced by the inhomogeneous crystallization of analytes in MALDI matrices [42], it possesses great application potential in glycopeptide identification and glycoprotein analysis for glycoproteomic study.

Acknowledgments

This work was financially supported by National Natural Science Foundation of China (21135002) and Priority Development Areas of The National Research Foundation for the Doctoral Program of Higher Education of China (20130091130005).

Appendix A. Supporting information

Supplementary data associated with this article can be found in the online version at http://dx.doi.org/10.1016/j.talanta.2016.09.012.

References

[1] R.G. Spiro, Glycobiology 22 (2002) 43R–56R.
[2] L. Lehle, S. Strahl, W. Tanner, Angew. Chem. Int. Ed. 118 (2006) 6956–6972.
[3] L. Lehle, S. Strahl, W. Tanner, Angew. Chem. Int. Ed. 45 (2006) 6802–6818.
[4] R.J. Woods, C.J. Edge, R.A. Dwek, Nat. Struct. Mol. Biol. 1 (1994) 499–501.
[5] P.M. Rudd, T. Elliott, P. Cresswell, I.A. Wilson, R.A. Dwek, Science 291 (2001) 2370–2376.
[6] L. Wells, K. Vosseller, G.W. Hart, Science 291 (2001) 2376–2378.
[7] K. Marino, J. Bones, J.J. Kattla, P.M. Rudd, Nat. Chem. Biol. 6 (2010) 713–723.
[8] D.F. Zielinska, F. Gnad, K. Schropp, J.R. Wisniewski, M. Mann, Mol. Cell 46 (2012) 542–548.
[9] M. Madera, Y. Mechref, M.V. Novotny, Anal. Chem. 77 (2005) 4081–4090.
[10] D. Ghosh, O. Krokhin, M. Antonovici, W. Ens, K.G. Standing, R.C. Beavis, J. A. Wilkins, J. Proteome Res. 3 (2004) 841–850.
[11] Y.W. Xu, Z.X. Wu, L.J. Zhang, H.J. Lu, P.Y. Yang, P.A. Webley, D.Y. Zhao, Anal. Chem. 81 (2009) 503–508.
[12] A. Dell, H.R. Morris, Science 291 (2001) 2351–2356.
[13] R. Chen, F. Wang, Y. Tan, Z. Sun, C. Song, M. Ye, H. Wang, H. Zou, J. Proteom. 75 (2012) 1666–1674.
[14] L. Wang, U.K. Aryal, Z. Dai, A.C. Mason, M.E. Monroe, Z.X. Tian, J.Y. Zhou, D. Su, K.K. Weitz, T. Liu, D.G. Camp II, R.D. Smith, S.E. Baker, W.J. Qian, J. Proteome Res. 11 (2012) 143–156.
[15] A. Halim, U. Ruetschi, G. Larson, J. Nilsson, J. Proteome Res. 12 (2013) 573–584.
[16] J.A. Ferreira, A.L. Daniel-da-Silva, R.M.P. Alves, D. Duarte, I. Vieira, L.L. Santos, R. Vitorino, F. Amado, Anal. Chem. 83 (2011) 7035–7043.
[17] W. Zhou, N. Yao, G.P. Yao, C.H. Deng, X.M. Zhang, P.Y. Yang, Chem. Commun. (2008) 5577–5579.
[18] D. Horak, L. Balonova, B.F. Mann, Z. Plichta, L. Hernychova, M.V. Novotny, J. Stulık, Soft Matter 8 (2012) 2775–2786.
[19] K. Sparbier, S. Kocb, I. Kessler, T. Wenzel, M. Kostrzewa, J. Biomol. Technol. 16 (2005) 407–413.
[20] C.-H. Yeh, S.-H. Chen, D.-T. Li, H.-P. Lin, H.-J. Huang, C.-I. Chang, W.-L. Shih, C.-L. Chern, F.-K. Shi, J.-L. Hsu, J. Chromatogr. A 1224 (2012) 70–78.
[21] T.H. Tran, S.Y. Park, H. Lee, S. Park, B. Kim, O.H. Kim, B.C. Oh, D. Lee, H. Lee, Analyst 137 (2012) 991–998.
[22] J. Zhu, F.J. Wang, K. Cheng, J. Dong, D.G. Sun, R. Chen, L.M. Wang, M.L. Ye, H. F. Zou, Proteomics 13 (2013) 1306–1313.
[23] G. Alvarez-Manilla, J.A. Atwood, Y. Guo, N.L. Warren, R. Orlando, M. Pierce, J. Proteome Res. 5 (2006) 701–708.
[24] H. Wan, J. Yan, L. Yu, Q. Sheng, X. Zhang, X. Xue, X. Li, X. Liang, Analyst 136 (2011) 4422–4430.
[25] Z.M. Guo, A.W. Lei, Y.P. Zhang, Q. Xu, X.Y. Xue, F.F. Zhang, X.M. Liang, Chem. Commun. (2007) 2491–2493.
[26] H.X. Huang, Y. Jin, M.Y. Xue, L. Yu, Q. Fu, Y.X. Ke, C.H. Chuang, X.M. Liang, Chem. Commun. (2009) 6973–6975.
[27] Y. Wada, M. Tajiri, S. Yoshida, Anal. Chem. 76 (2004) 6560–6565.
[28] A.J. Shen, Z.M. Guo, L. Yu, L.W. Cao, X.M. Liang, Chem. Commun. 47 (2011) 4550–4552.
[29] Z.C. Xiong, Y.S. Ji, C.L. Fang, Q.Q. Zhang, L.Y. Zhang, M.L. Ye, W.B. Zhang, H. F. Zou, Chem. Eur. J. 20 (2014) 7389–7395.
[30] Q. Zhang, A.A. Schepmoes, J.W. Brock, S. Wu, R.J. Moore, S.O. Purvine, J. W. Baynes, R.D. Smith, T.O. Metz, Anal. Chem. 80 (2008) 9822–9829.
[31] L. Zhang, Y. Xu, H. Yao, L. Xie, J. Yao, H. Lu, P. Yang, Chem. Eur. J. 15 (2009) 10158–10166.
[32] R. Ma, J.J. Hu, Z.W. Cai, H.X. Ju, Nanoscale 6 (2014) 3150–3156.
[33] X. Sun, R. Liu, X. He, L. Chen, Y. Zhang, Talanta 81 (2010) 856–864.
[34] X.D. Yuan, J. Shen, G.H. Li, J.M. Kim, S.E. Park, Chin. J. Catal. 25 (2002) 435–438.
[35] D. Zhao, J. Feng, Q. Huo, N. Melosh, G.H. Fredrickson, B.F. Chmelka, G.D. Stucky, Science 279 (1998) 548–552.
[36] R. Bal, S. Sivasanker, Appl. Catal. A 24 (2003) 373–382.
[37] Y. Zheng, X.W. Su, X.H. Zhang, W. Wei, Y.H. Sun, in: Nanoporous Materials IV, 156, 2005, pp. 205–212.
[38] D.W. Qi, H.Y. Zhang, J. Tang, C.H. Deng, X.M. Zhang, J. Phys. Chem. C 114 (2010) 9221–9226.
[39] J.J. Hu, R.N. Ma, F. Liu, Y.L. Chen, H.X. Ju, RSC Adv. 4 (2014) 28856–28859.
[40] Y.Y. Qu, J.X. Liu, K.G. Yang, Z. Liang, L.H. Zhang, Y.K. Zhang, Chem. Eur. J. 18 (2012) 9056–9062.
[41] L. Liu, Y. Zhang, L. Zhang, G. Yan, J. Yao, P. Yang, H. Lu, Anal. Chim. Acta 753 (2012) 64–72.
[42] J.J. Hu, F. Liu, H.X. Ju, Anal. Chem. 87 (2015) 4409–4414.